Implementation of the Doppler Shift Attenuation Method using TIP/TIGRESS at TRIUMF

Jonathan Williams

PhD Candidate
Simon Fraser University - Department of Chemistry

CAP Congress 2017
May 29, 2017

Gamma-ray spectroscopy and nuclear structure

- Study of electromagnetic transition rates and energies via gamma-ray spectroscopy can yield information on nuclear structure.
- Eg. $B(E2)$ measurements to determine the deformation in a nuclear charge distribution β:

$$\frac{1}{\tau E_{\gamma}^{5}} \propto B(E2) \propto \beta^{2}$$

- E_{γ} can be measured with high precision via gamma-ray spectroscopy.
- τ measurable via RDM ($\tau > 1$ ps), DSAM ($\tau < 1$ ps).

Doppler Shift Attenuation Method (DSAM)

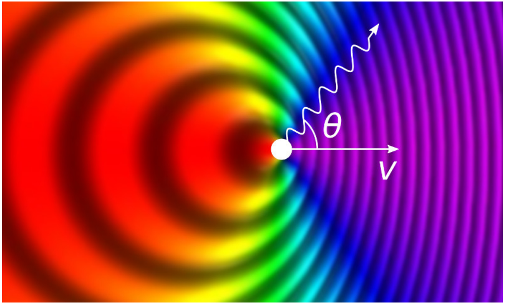

$$E_\gamma = E_0 \frac{\sqrt{1-\beta^2}}{1-\beta cos\theta}, \quad \beta = \frac{v}{c}$$

Detected gamma-ray energy depends on the speed of the residual nucleus at decay time.

- Can infer the lifetime of the state being measured from the gamma-ray energy distribution.

Doppler Shift Attenuation Method (DSAM)

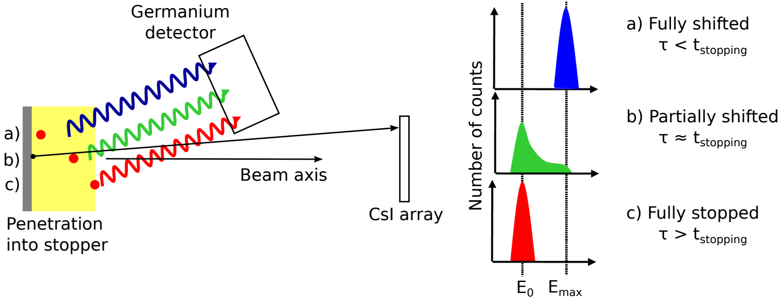

- Nucleus of interest slows and stops in a thick target backing.
- Observe lineshape depending on the speed distribution of the residual at time of gamma-ray emission.

Fusion-evaporation reaction mechanism

- A compound system forms with large angular momentum and recoil speed.
- The system decays first by the emission of particles (forming species of interest).
- Residual nucleus (species of interest) decays by gamma-ray emission.

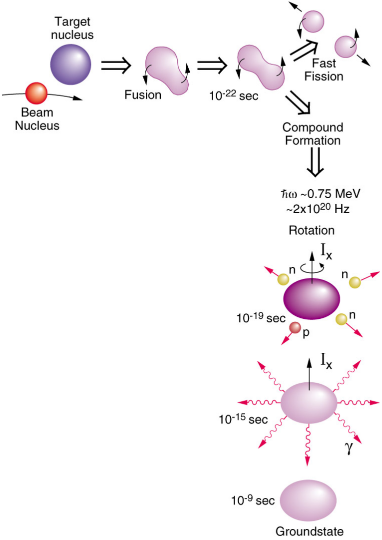

TIP experimental setup

Gamma ray detection: TIGRESS (all 16 clovers usable)

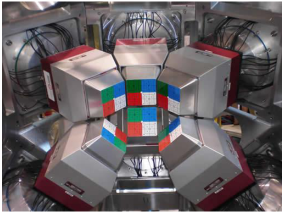

Charged particle detection: CsI(Tl) detectors, 2 configurations:

- 24 element wall (pictured)
- Ball with $\sim 3\pi$ spherical coverage (under construction).

+ the TIP DSAM target device.

TIP chamber in TIGRESS

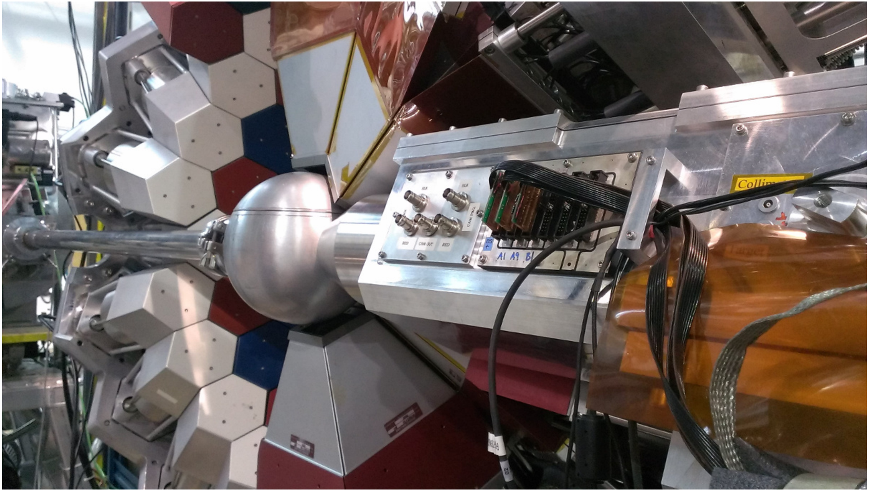

P. Voss et al. Nucl. Inst. Meth. A **746** 87 (2014)

TIP DSAM configuration

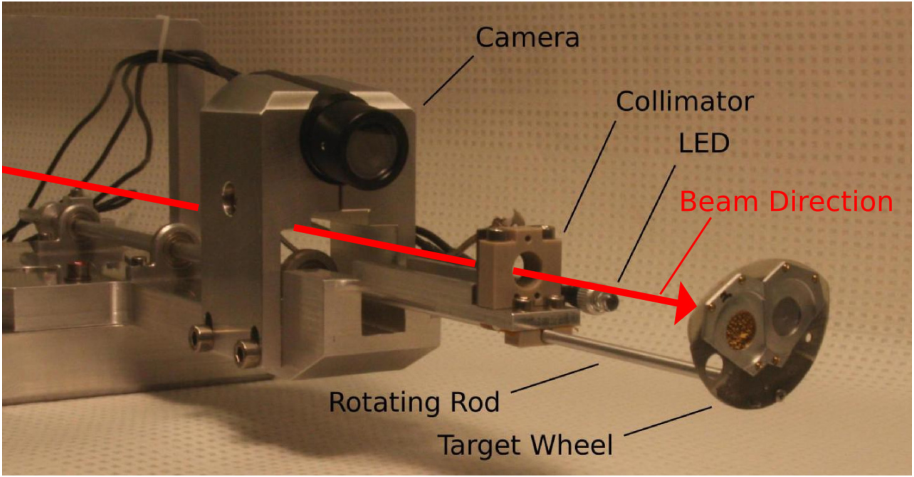

P. Voss et al. Nucl. Inst. Meth. A **746** 87 (2014)

TIP target position

P. Voss et al. Nucl. Inst. Meth. A **746** 87 (2014)

TIP/TIGRESS Commissioning experiment

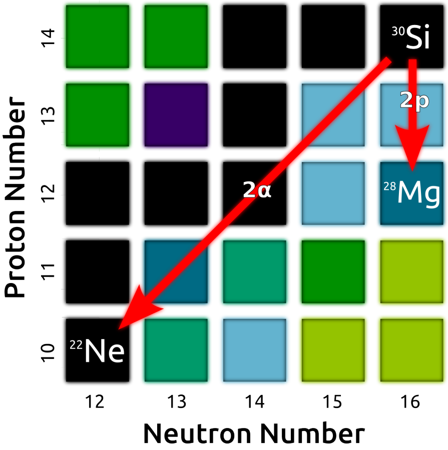

TIGRESS/TIP @ TRIUMF:

- ^{18}O beam (48 MeV)
- $^{nat.}C$ target (0.433 mg/cm^2), Au backing (28.79 mg/cm^2)[1]
- CsI(Tl) detector wall

Particles evaporate from the ^{30}Si compound nucleus to form various residual species.

- Mostly observed ^{22}Ne.

[1] J. Greene et al. J. Radioanal. Nucl. Chem. **299** 1121 (2014)

^{22}Ne lineshapes

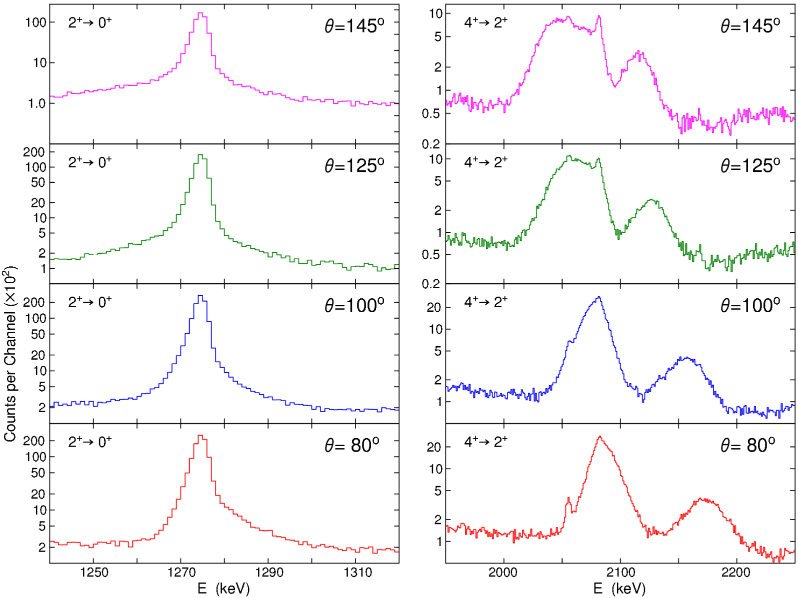

Doppler shift lineshape analysis

- Want to determine lifetimes of transitions from their lineshapes, which arise from the Doppler shift distribution of recoiling nuclei
- Many factors influence this...
  - Momentum of incoming beam
  - Momentum distribution of particles evaporated after reaction
  - Distribution of reaction positions within the target
  - Stopping of beam and reaction products inside the target/stopper
  - Geometry of the detector system(s) with respect to the reaction target
  - Other annoying things such as detection efficiencies
  - ...
  - Lifetime of the transition

Parameter space is way too large to solve analytically
$\rightarrow$ need to simulate the process!

Doppler shift lineshape analysis code

- GEANT4[1] based analysis code to extract lifetimes from DSAM lineshapes was developed, including:
    - Target, stopper, and detection system geometry
    - Fusion-evaporation reaction kinematics
- Additional code for comparing lineshapes between simulation and experiment using χ^2 analysis has been developed.

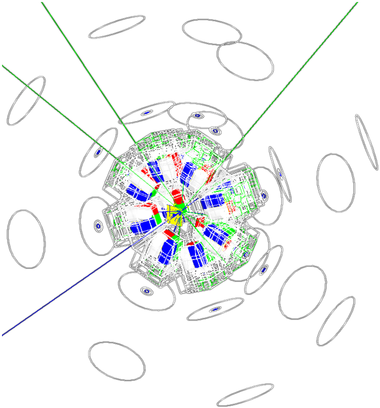

[1]S. Agostinell, et al., Nucl. Instr. Meth. Phys. Res. A 506 250303 (2003).

Fusion Evaporation in GEANT4

- Formation of compound system at a random depth in the target, followed by emission of one or more particles.
- Gamma-ray emission from the residual nucleus according to user defined lifetime.
  - GEANT4 handles particle momenta and Doppler shift of gamma rays.
  - Sequential gamma ray emission is possible (cascades).

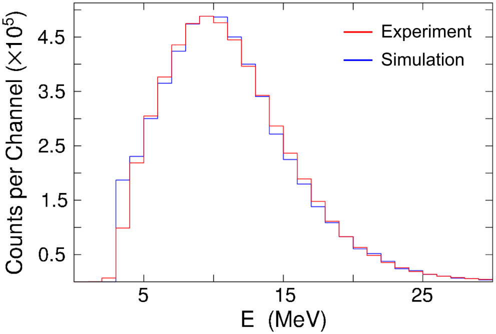

- Evaporated particle energy distribution modelled to match experiment (Gaussian with exponential tail).

Lineshape vs. lifetime

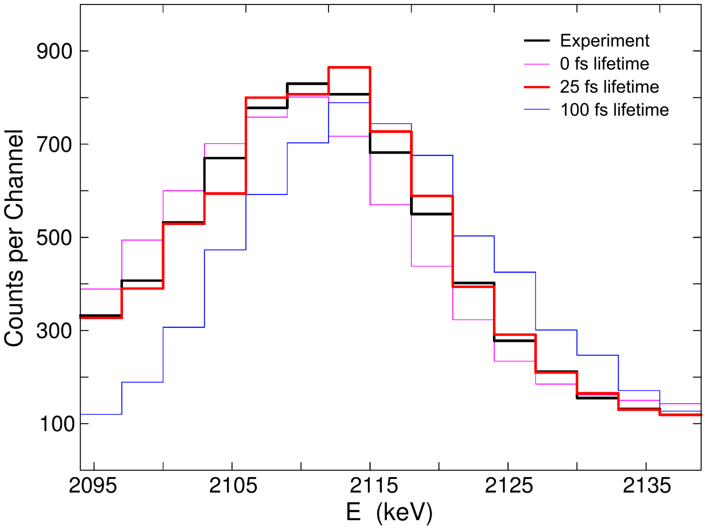

Peak shape vs. simulated lifetime for the 5523 keV level in ^{22}Ne.

χ^2 statistic

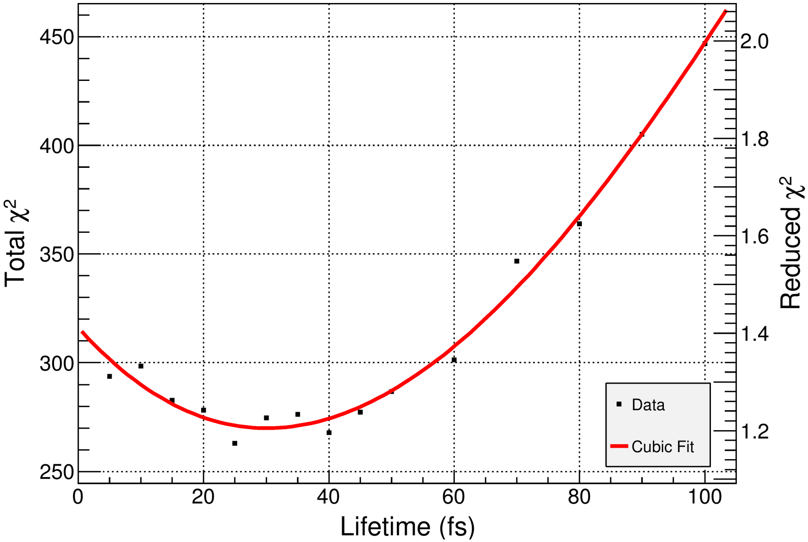

χ^2 statistic vs. simulated lifetime for the 5523 keV level in ^{22}Ne.

χ^2 statistic

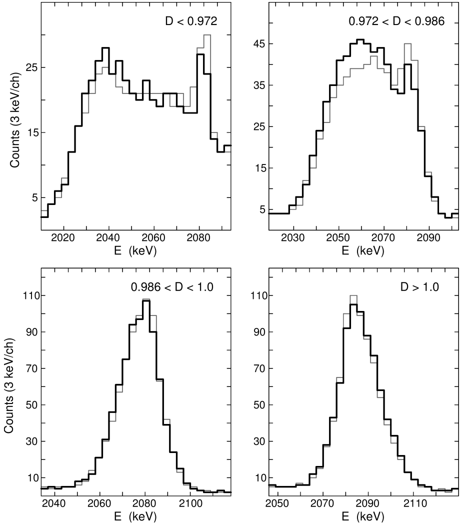

Best fit simulated lineshapes for the 3357 keV level in ^{22}Ne at various Doppler Shift factors.

Lifetimes in ^{22}Ne

Measured lifetimes for select observed ^{22}Ne transitions.

Evaluated E_{level} (keV)[1]	$J\pi$[1]	Evaluated τ (fs)[1]	Measured τ (fs)
3357.2	$4+$	324(6)	290(50)
5146.0	$2-$	1200(300)	1100(200)
5523.3	$(4)+$	30(4)	30(10)
6311.0	$(6+)$	71(6)	70(5)
6345.1	$4+$	19(4)	11(6)
7423.0	$(5+)$	< 4	5(11)
8976	-	-	< 6

[1] M. S. Basunia, Nuclear Data Sheets 127 (2015) 69–190.

Analysis summary

Analysis of ^{22}Ne from the commissioning run data is complete.

- Tools appear to be functioning well, are designed to be extendable to future experiments.

Detailed paper on analysis technique has been published:

Nuclear Instruments and Methods in Physics Research Section A: Accelerators, Spectrometers, Detectors and Associated Equipment

Volume 859, 1 July 2017, Pages 8–17

Implementation of the Doppler shift attenuation method using TIP/TIGRESS at TRIUMF: Fusion-evaporation lifetime measurements in ^{22}Ne

J. Williams[a], C. Andreoiu[a], R. Ashley[a], G.C. Ball[b], T. Ballast[b], P.C. Bender[b], C. Bolton[c], V. Bildstein[d], A. Chester[a], D.S. Cross[a], T. Domingo[a], T. Drake[e], A. Garnsworthy[b], P. Garrett[d], B. Hadinia[d], G. Hackman[b],

Show more

Further developments

1) CsI ball construction

2) ^{40}Ca target development

TIP CsI ball

Spherical array which replaces the 24-element wall.

- 128 detectors in 10 rings.
- Total array gives $\sim 3\pi$ coverage.

The first 4 rings (38 detectors) have been tested in beam.

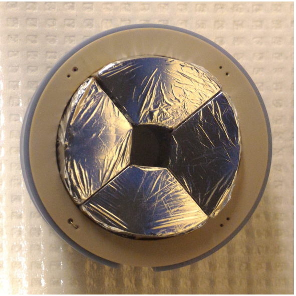

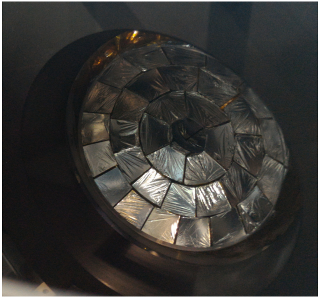

TIP CsI ball design

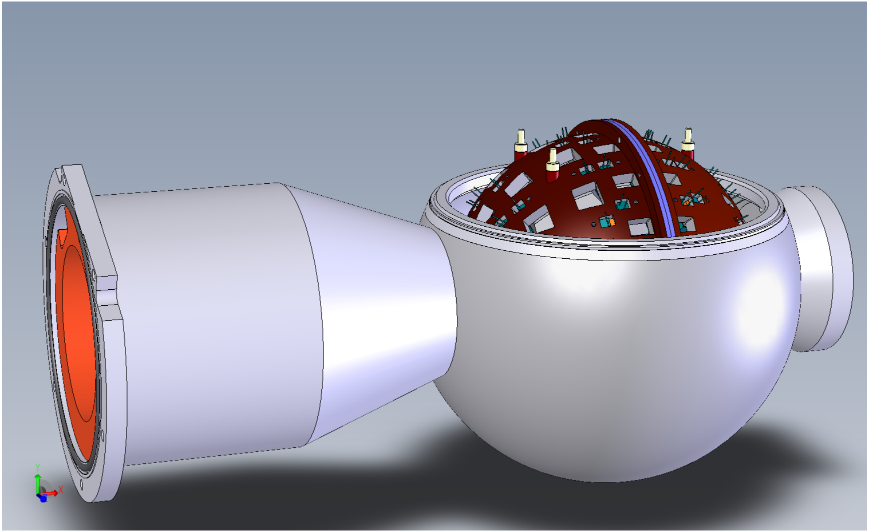

TIP CsI ball design

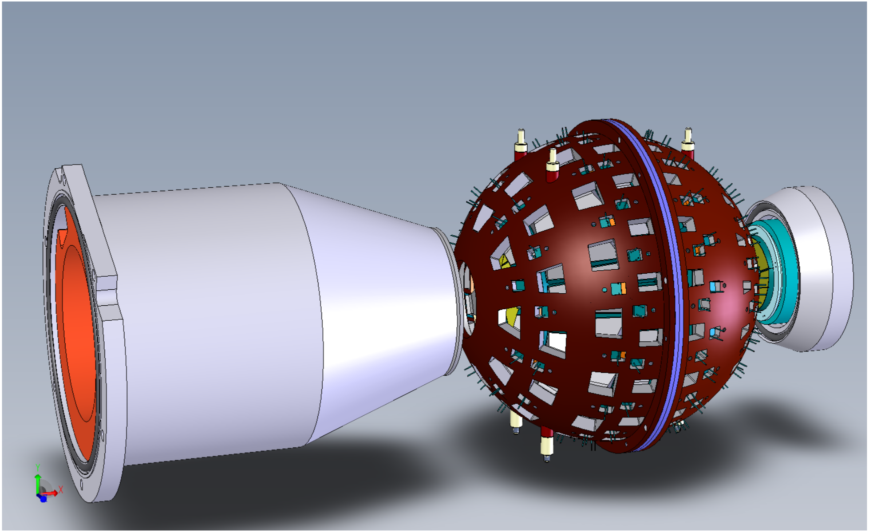

TIP CsI ball design

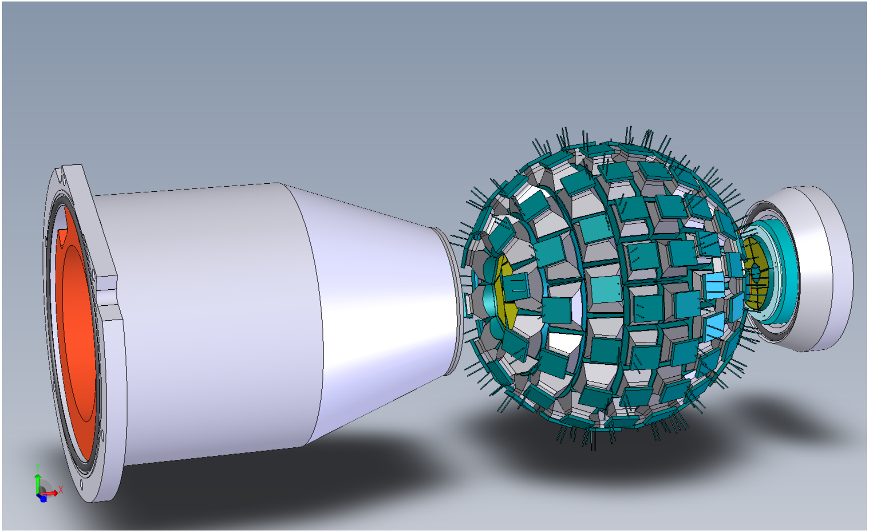

TIP CsI ball design

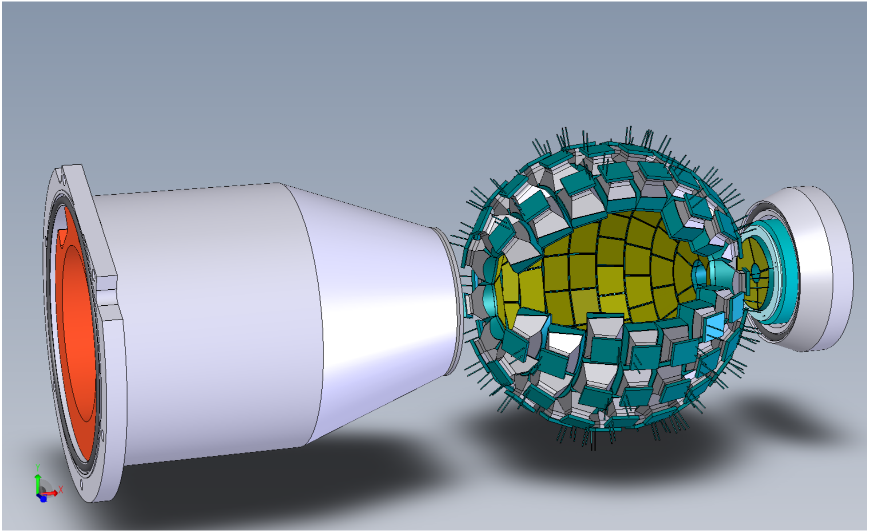

^{40}Ca targetry

^{40}Ca is the heaviest stable $N = Z$ species - would be a very useful target material for studies of proton rich species.

Unfortunately, chemistry isn't on our side:

- Calcium oxidizes spontaneously and rapidly:

$$2\ \mathrm{Ca}\ (s) + \mathrm{O_2}\ (g) \rightarrow 2\ \mathrm{CaO}\ (s)$$

- Earth has a lot of oxygen in its atmosphere.
- Fusion reactions on oxygen have high cross sections and contaminate measurements.

^{40}Ca targetry (cont.)

Evaporator provided by TRIUMF detector lab for target production.

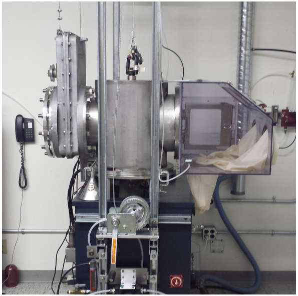

- Dual-boat: can evaporate calcium and protective layer material without breaking vacuum.
- Can be vented to argon rather than air.

Developed protected Ca targets:

- Gold foil backing.
- Calcium spot at center (5mm diameter, $\sim$1 mg/cm^2).
- Gold protective layer ($\sim$0.2 mg/cm^2) covering frame.

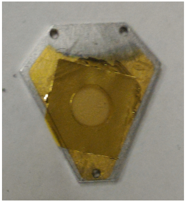

Target test results

Looked for ^{4}He fusion on various targets.

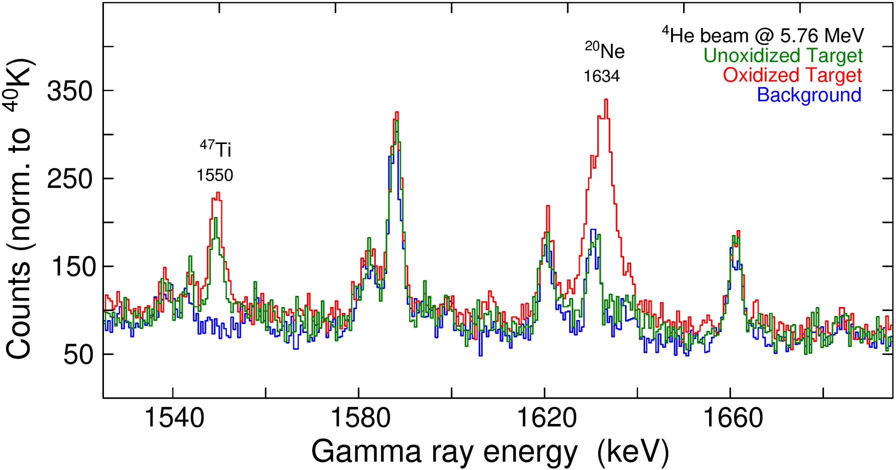

Future Work

Will run an experiment studying $N = Z$ ^{68}Se via ^{40}Ca(^{36}Ar,2α)^{68}Se.

- Planned for this fall.

Possible future directions:

- Analysis of ^{28}Mg data.
- Use of calcium target to study other nuclei.
  - ^{55,56}Ni ($N = Z = 28$ region) via ^{20}Na + ^{40}Ca fusion-evaporation.
  - Heavy proton-rich species using other proton-rich RIBs.

Acknowledgements

Simon Fraser University
Current: A. Chester, T. Domingo, K. Starosta
Former: R. Ashley, U. Rizwan, P. Voss
Other Groups: C. Andreoiu, D. S. Cross

SFU Science Machine & Electronics Shops
R. Holland, P. Kowalski, J. Shoults, K. Van Wieren

TRIUMF
G. Ball, T. Ballast, P. C. Bender, C. Bolton, A. Garnsworthy, G. Hackman, R. Henderson, R. Krücken, D. Miller, W. J. Mills, M. Moukaddam, M. Rajabali, C. Unsworth, Z.-M. Wang

University of Guelph
V. Bildstein, P. Garrett, B. Hadinia, D. Jamieson, B. Jigmeddorj, C. E. Svensson, A. D. Valera, J. Wong

University of Liverpool
C. Unsworth

University of Surrey
A. Knapton

University of Toronto
T. Drake

Analysis code used in this project is available at **github.com/SFUNUSC**

Stopping power comparison

Comparison of simulations using stopping powers from ICRU73[1] (GEANT4 default) and SRIM[2] was performed.

For transitions with short lifetimes (< 0.2 ps) the effect on the source speed distribution is $\leq 10\%$.

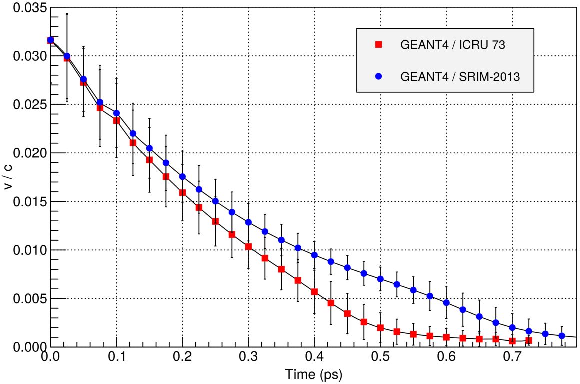

Residual nucleus speed in gold as a function of stopping time. Initial residual energy distribution taken from full simulations.

[1] ICRU Report 73, J. ICRU **5(1)** 1 (2005)
[2] J. Ziegler et al., Nucl. Instr. Meth. Phys. Res. B **268** 1818 (2010)

April target test results

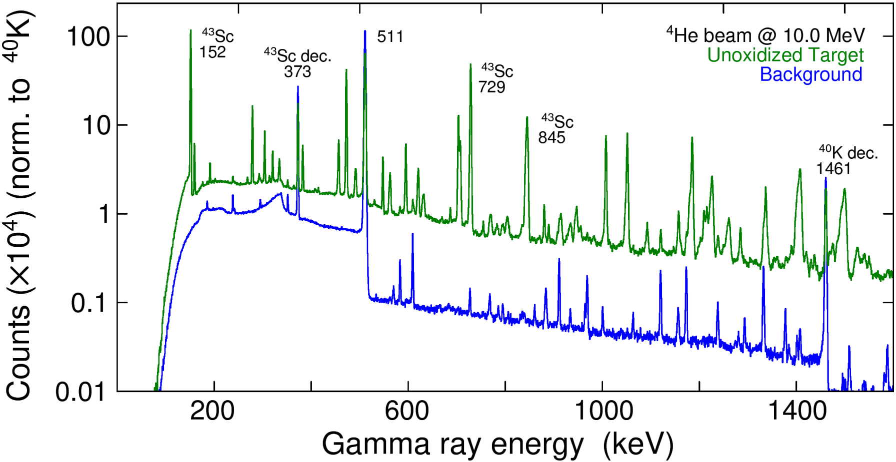

April target test results

Protected target:

- No evidence of reactions on oxygen.
- No visible change in the target surface during the run.
- $^{16}O/^{40}Ca$ number density based on PACE4 cross-sections: $<0.15\%$
  - From observed production of ^{20}Ne, ^{44}Ti.
  - Compared to 7.0% from previous run.

Exposed (oxidized) target:

- Exposed to atmosphere for 2 days before running.
- Production of ^{20}Ne from alpha fusion on oxygen observed.
- $^{16}O/^{40}Ca$ number density based on PACE4 cross-sections: 3.4%

Alpha energy loss in calcium

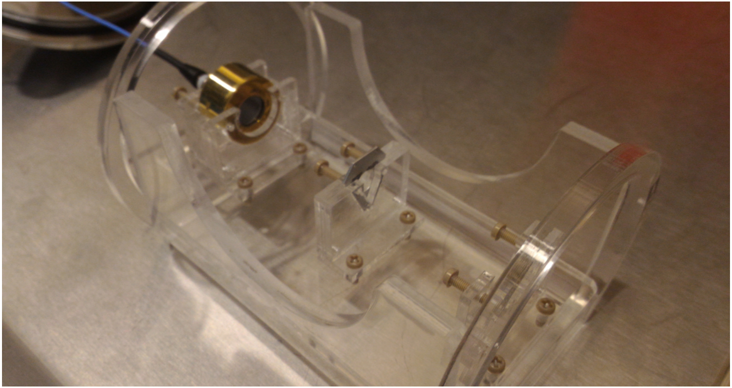

Investigated energy loss of alpha particles in calcium targets, in order to determine thickness of calcium layer based on known stopping powers.

- ^{241}Am source, target, and Si detector in fixed geometry.
- Thin mylar target backing used to allow alpha transmission.

Alpha energy loss in calcium

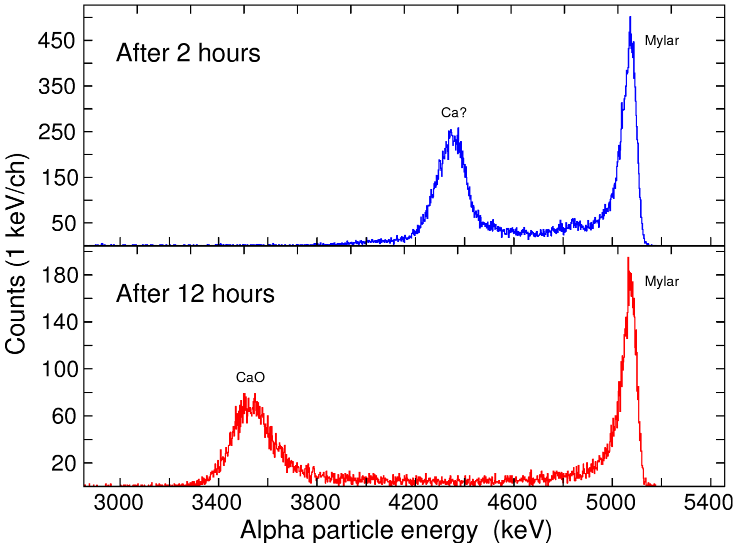

Work to measure oxidation kinetics underway...

Shape coexistence along the $N = Z$ line

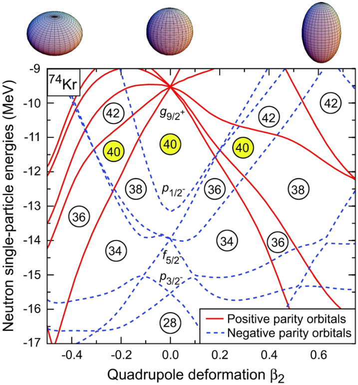

A. N. Andreyev et al. Nature **405** 430 (2000).

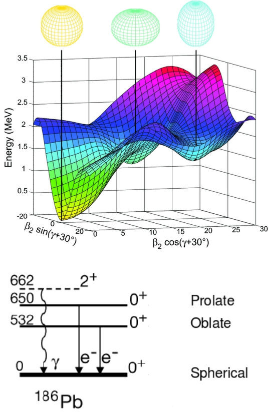

- Nearly degenerate shell gaps exist for positive and negative quadrupole deformations leading to shape coexistence.

Studying nuclear structure using the electromagnetic force

- The electromagnetic force provides a convenient non-intrusive probe of nuclear systems bound by the strong force.
- Lifetime measurements using gamma-ray spectroscopy provide:
  1. An observable sensitive to nuclear structure.
  2. A sensitive benchmark for nuclear model calculations.

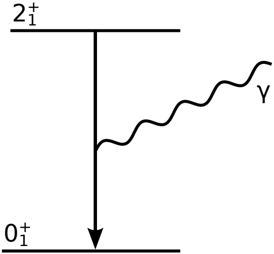

$$\tau(E2; 2_1^+ \rightarrow 0_1^+) = \lambda(E2; 2_1^+ \rightarrow 0_1^+)^{-1}$$

$$\lambda(E2; 2_1^+ \rightarrow 0_1^+) \propto E(2_1^+)^5 \times B(E2; 2_1^+ \rightarrow 0_1^+)$$

$$B(E2; 2_1^+ \rightarrow 0_1^+) = \frac{1}{5} \left| \langle 2_1^+ | \, |E2| \, | 0_1^+ \rangle \right|^2 \propto \beta^2$$

Recent studies in $N = Z = 34$ ^{68}Se

Model calculations

Model	Shell Model	Interacting Boson Model	Hartree-Bogoliubov	Self-consistent Collective Coordinate		Excited Vampir
$B(E2, 2_1^+ \to 0_1^+)$ [e^2fm^4]	100[1]	280[2]	500[3]	725[4]	834[4]	1048[5]

[1]M. Hasegawa et al. Phys. Lett. B **656** 51 (2007).; [2]F. Il. Khudair, Y. S. Li, G. L. Long, Phys. Rev. C **75** 054316 (2007).
[3]T. A. War et al. Eur. Phys. J. A **22** 13 (2004).; [4]N. Hinohara et al. Prog. Theor. Phys. (Kyoto) **119** 59 (2008).
[5]A. Petrovici et al. Nucl. Phys. A **710** 246 (2002).

Recent measurements

Method	$B(E2, 2_1^+ \to 0_1^+)$ [e^2fm^4]	τ [ps]
Coulomb Excitation[6]	430(60)	4.2(6)
Recoil Distance Method[7]	390(70)	4.6(8)

[6]A. Obertelli et al. Phys. Rev. C **80** 031304(R) (2009).
[7]A. J. Nichols et al. Phys. Rev. B **733** 52 (2014)

^{22}Ne level scheme

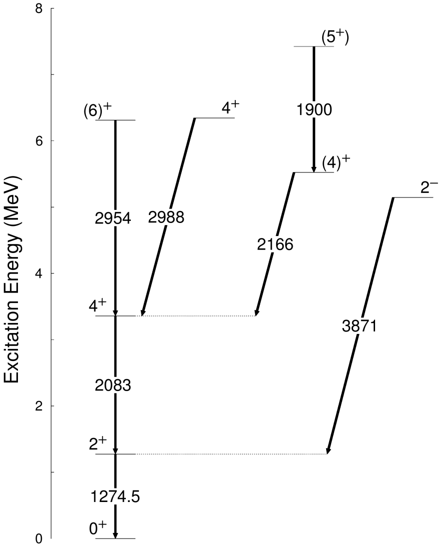

Semiconductor detector (eg. HPGe) schematic

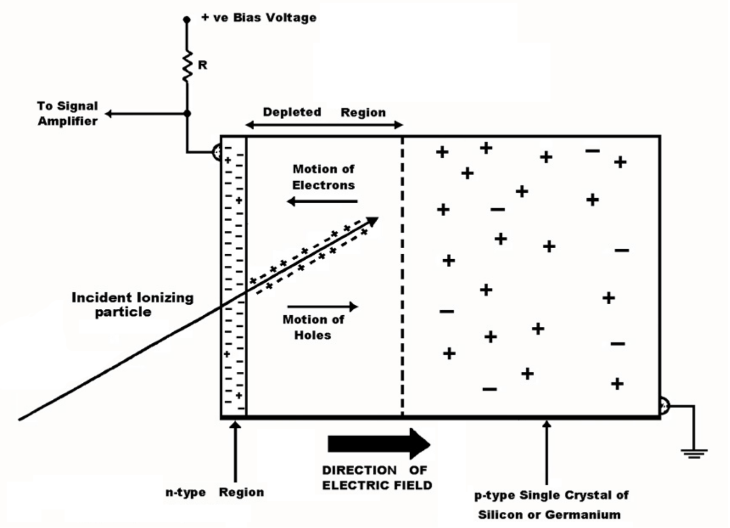

Relativistic Doppler effect

For photons:
$E = hf$ (energy)
$\lambda = c/f$ (wavelength)
$T = 1/f$ (wave period)

Other definitions:
$\beta = v/c$
$\gamma = \frac{1}{\sqrt{1-\beta^2}}$

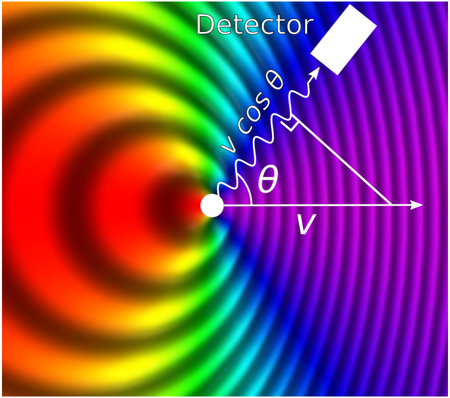

From non-relativistic Doppler shift:

$$\lambda_{obs} = \frac{c}{f_{obs}} = \frac{c - v_{||}}{f_{src}} = \frac{c - v_{src} cos\theta}{f_{src}}$$

$$\frac{f_{obs}}{f_{src}} = \frac{T_{src}}{T_{obs}} = \frac{c}{c - v_{src} cos\theta} = \frac{1}{1 - \beta cos\theta}$$

Relativistic Doppler effect (cont.)

From time dilation (special relativity):

$$T_{src} = \frac{T_{obs}}{\gamma}, \gamma = \frac{1}{\sqrt{1-\beta^2}}$$

$$\frac{f_{obs}}{f_{src}} = \frac{T_{src}}{T_{obs}} = \frac{1}{\gamma} = \sqrt{1-\beta^2}$$

Combining Doppler shift and time dilation:

$$\frac{f_{obs}}{f_{src}} = \frac{\sqrt{1-\beta^2}}{1-\beta cos\theta}$$

$$E_{obs} = E_{src}\frac{\sqrt{1-\beta^2}}{1-\beta cos\theta}$$

Semi-empirical mass model[1]

Model treating the nucleus like a liquid drop, with shell model correction terms:

$$BE(A,Z) = a_V A - a_s A^{2/3} - a_c \frac{Z(Z-1)}{A^{1/3}} - a_A \frac{(A-2Z)^2}{A} + \Delta E_{pair}$$

Deformation from sphericity affects the surface and Coulomb terms, eg. for ellipsoidal deformation:

$$a_s A^{2/3} \rightarrow a_s A^{2/3}(1 + (2/5)\epsilon^2)$$

$$a_c \frac{Z(Z-1)}{A^{1/3}} \rightarrow a_c \frac{Z(Z-1)}{A^{1/3}}(1 - (1/5)\epsilon^2)$$

$$\epsilon = \sqrt{1 - b^2/a^2} \text{ (minor/major axis length ratio)}$$

[1] K. Heyde, Basic Ideas and Concepts in Nuclear Physics, IOP Publishing, 2004.

Nuclear shell model

Similar to electron shell model. Main differences:

- Flat-bottom potential representing nuclear interaction.
- Protons and neutrons have their own shells.
- Strong spin-orbit coupling results in different magic numbers.
  - Due to spin dependence of the nuclear interaction, from coupling of a nucleon's spin and its orbital angular momentum (which depends on the mean field produced by all nucleons).

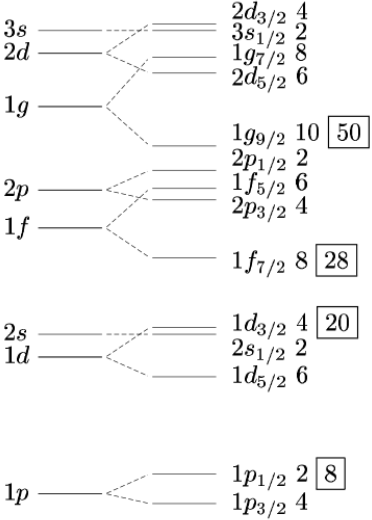

Fermi's golden rule

Transition rate depends on initial and final wavefunctions, interaction V_p which causes the transition, and density of final states $\rho(E_f)$.

$$\lambda = \frac{2\pi}{\hbar} \left| \int \psi_f^* V_p \psi_i dv \right|^2 \rho(E_f)$$
$$\propto \left| \langle \psi_f | \, V_p \, | \psi_i \rangle \right|^2$$

So for an E2 transition:

$$\lambda \propto \frac{1}{5} \left| \langle 2_1^+ | \, |E2| \, | 0_1^+ \rangle \right|^2 = B(E2; 2_1^+ \rightarrow 0_1^+)$$

Weisskopf estimates[1]

Estimates of reduced transition probabilities assuming a single particle transition and nucleus with uniform density, radius $R = r_0 A^{1/3}$.

$$B(EL) = \frac{1}{4\pi}\left[\frac{3}{L+3}\right]^2 (r_0)^{2L} A^{2L/3} \ \ [e^2 fm^{2L}]$$

$$B(ML) = \frac{10}{\pi}\left[\frac{3}{L+3}\right]^2 (r_0)^{(2L-2)/2} \mu_n^2 \ \ [e^2 fm^{2L-2}]$$

μ_n - magnetic moment of particle of interest.

[1] W. Loveland, D. J. Morrissey, G. T. Seaborg, Modern Nuclear Chemistry, Wiley, 2006.

Nuclear charge distribution[1]

Potential arising from charge distribution $\rho(\vec{r})$ of nucleons at a distance $\vec{R}$:

$$\Phi(\vec{R}) = \frac{1}{4\pi\epsilon_0}\int_{Vol}\frac{\rho(\vec{r})}{|\vec{R}-\vec{r}|}d\vec{r}$$

Expanded in $|\vec{r}/\vec{R}|$:

$$\Phi(\vec{R}) = \frac{1}{4\pi\epsilon_0}q/R + \sum_i \frac{p_i}{4\pi\epsilon_0}\frac{X_i}{R^3} + \sum_{ij}\frac{1}{2}\frac{1}{4\pi\epsilon_0}\frac{Q_{ij}}{R^5}X_iX_j + ...$$

$$p_i = \int \rho(\vec{r})x_i d\vec{r},$$
$$Q_{ij} = \int \rho(\vec{r})(3x_ix_j - r^2\delta_{ij})d\vec{r}.$$

with $i = 1,2,3$ corresponding to Cartesian coordinates x, y, z.

[1] K. Heyde, Basic Ideas and Concepts in Nuclear Physics, IOP Publishing, 2004.